IEEE Access
Multidisciplinary ⋮ Rapid Review ⋮ Open Access Journal

Received April 20, 2018, accepted June 5, 2018, date of publication June 19, 2018, date of current version July 25, 2018.

Digital Object Identifier 10.1109/ACCESS.2018.2848899

Resource Split Full Duplex to Mitigate Inter-Cell Interference in Ultra-Dense Small Cell Networks

HAESOON LEE[1], (Student Member, IEEE), YOSUB PARK[2], (Member, IEEE), AND DAESIK HONG[1], (Senior Member, IEEE)

[1]Information Telecommunication Laboratory, School of Electrical and Electronic Engineering, Yonsei University, Seoul 03722, South Korea
[2]Autonomous Machine Laboratory, AI Center, Samsung Research, Samsung Electronics Company, Seoul 06765, South Korea

Corresponding author: Daesik Hong (daesikh@yonsei.ac.kr)

This work was supported in part by the National Research Foundation of Korea Grant through the Korea Government (MSIT) under Grant 2018R1A2A1A05021029 and in part by the Institute for Information and Communications Technology Promotion Grant through the Korea Government (MSIP) (Development on the core technologies of transmission, modulation and coding with low-power and low-complexity for massive connectivity in the IoT environment) under Grant 2016-0-00181.

ABSTRACT When a full duplex (FD) system is used in a multi-cell environment, the simultaneous transmission and reception cause an increase in inter-cell interference compared with half duplex (HD) systems. This problem is more severe in ultra-dense small cell network (UDN) environments where small cells are extremely dense. Therefore, the performance gain of FD transmission over traditional HD transmission is significantly degraded by this increase in inter-cell interference. To overcome the performance loss, we consider a new FD operation that can avoid the increased inter-cell interference caused by FD use. The basic idea involves separating the small cell base stations into two groups and using half of the communication resources in a manner similar to HD systems. We compare the performance of conventional HD and FD with the proposed scheme in terms of network throughput. Network throughput physically refers to the total throughput per unit area of the network. The simulation results consider indoor and outdoor scenarios and show that our proposed scheme outperforms conventional FD and conventional HD.

INDEX TERMS Full-duplex, ultra-dense small cell network, inter-cell interference, network throughput, indoor environment, outdoor environment.

I. INTRODUCTION

Full duplex (FD) systems have recently been receiving significant attention from academia and industry as an attractive option for 5G technology. Compared to half duplex (HD) systems, in-band FD systems simultaneously transmit and receive data on the same frequency band [1], [2]. Ideally, FD transmission should be able to double spectral efficiency compared to conventional HD transmission [3].

In addition, ultra-dense small cell networks (UDN) are considered to be one of the key directions for 5G technology. It is predicted that the UDN concept will be applied after 2020 [4]–[7]. A massive number of small cells will then be deployed horizontally and vertically.

If the FD system is used in a UDN, the FD transmitter can communicate using a small amount of transmit power due to the short cell range of the small cell. With this small transmit power, reducing self-interference (SI) to noise levels becomes much easier. In these FD UDNs, inter-cell interference is more dominant than SI. In particular, due to the simultaneous transmission and reception, the number of streams of inter-cell interference in the FD UDN is twice that in the HD UDN.

Several works have been published in academia on efforts related to the FD UDN [8]–[12]. In [8], the throughput of the FD multi-cell is compared with that of the HD multi-cell, and the HD outperforms the FD due to multiple-input multiple-output (MIMO) spatial multiplexing gains. Also, the impact of the doubled inter-cell interference on FD small cell networks is shown in [9], where an advanced interference suppression receiver is considered as an approach for removing its heavy impact. In [10]–[12], FD performance in UDNs is investigated with system level simulation. System level results indicate that there is a trade-off between the MIMO spatial multiplexing of HD systems and the simultaneous transmission and reception of FD systems [10]. In [11], a system level simulator with real channel measurements is used to estimate the effective performance gain of FD compared with traditional HD in a real scenario of dense small cells. In [12], the SI cancellation capabilities are shown using a real demonstrator and these results are reflected in system level results. A common finding throughout these studies is that the performance gain of FD over traditional HD transmission is significantly degraded by the increase in inter-cell interference due to the simultaneous transmission and reception.

The studies we introduced above show the performance limitation of FD in terms of throughput. Therefore, we propose a new FD operation that can overcome the performance limitations of the FD in the interference-limited environment. The basic idea underlying the proposed scheme involves separating the small cell base stations (BS) into two groups to reduce the number of interference streams compared to conventional FD. We use network throughput to evaluate the performance of the UDN. Network throughput physically refers to the total throughput per unit area of the network. Simulation results where we considered indoor and outdoor scenarios show that our proposed scheme outperforms conventional FD and conventional HD.

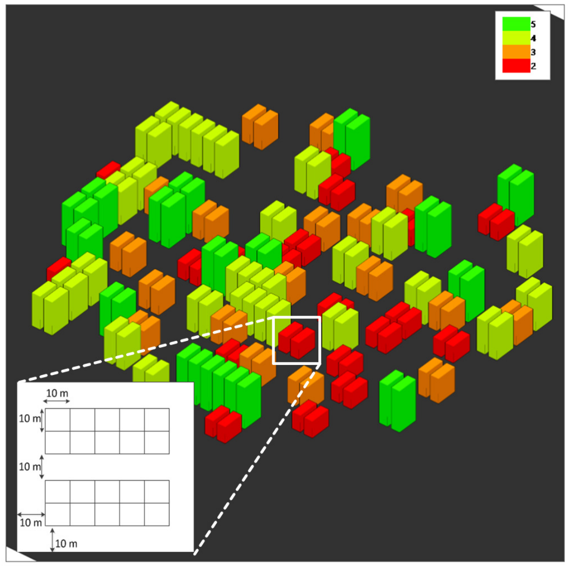

FIGURE 1. 3GPP dual-stripe urban indoor model.

II. SYSTEM MODEL

A. ULTRA-DENSE SMALL CELL NETWORKS

We consider a UDN [4], where the BSs are distributed according to a stationary process Π_B with spatial density λ in a finite two-dimensional plane. Macro BSs are layered with small cells. We consider the *Cell Type* 3 scenario described in [13], which means the macro BSs use different frequency bands than the small cell BSs. The macro BSs are thus outside the scope of this work. The term 'BS' used hereinafter refers to a small cell BS.

In this paper, two different BS deployment scenarios are considered for the UDN - indoor and outdoor scenarios [4], [6]. The indoor scenario is defined as one where low-powered indoor small cells like femto cells are deployed by individual users or enterprises in indoor settings. The outdoor scenario is defined as a situation involving high-powered outdoor small cells like pico cells installed by mobile operators. In these scenarios, the small cell BSs have low computing power compared with the macro cell BSs and have a backhaul link to the core networks via consumer broadband connections such as digital subscriber lines (DSL), cable, or fiber.

For the indoor scenario, we consider the dual-stripe urban model with random number of uniform floors between 2 and 5 to reflect indoor propagation and penetration loss by multiple walls [14]. As shown in Fig. 1, each floor has two stripes of apartments, with 10 rooms for each stripe. The size of a single room is 10 m × 10 m, and there is a street between the two stripes of apartments that is 10 m in width. In this way, we can model a single building with a random number of uniform floors between 2 and 5. To place each building, we consider the Qualcomm indoor model [5]. We make a square grid with distance 60 m and randomly select building position from the points on the grid with spatial density λ_{BL}, where λ_{BL} means the number of buildings per unit area. The BSs are uniformly distributed inside the apartments. Each BS has at least one user equipment (UE) within the same apartment and the set of the UEs is denoted as Π_U.

We use Keenan-Motley multi-wall models for indoor propagation and penetration loss by multiple walls [5], [14]. The pathloss between transmitter and receiver in the same and a different building can be given by, respectively,

$$l_{in,s}^{(\mathrm{dB})}(d) = 43.26 + 20\log_{10}(10d) + 0.5\chi + q_{iw}L_{iw}, \quad (1)$$

$$l_{in,d}^{(\mathrm{dB})}(d) = \max(20.1 + 37.6\log_{10}(10d), 43.26) + 20\log_{10}(10d) + 0.5\chi + q_{iw}L_{iw} + q_{ow}L_{ow}, \quad (2)$$

where d is the distance between transmitter and receiver in meters; χ is a random variable with uniform distribution (0, 25); L_{iw} and L_{ow} are inner wall and outer wall penetration losses, respectively; q_{iw} and q_{ow} are the number of inner walls and outer walls between the transmitter and receiver. The ceiling between the floors is considered to be an inner wall.

For the outdoor scenario, we consider the Poisson point process (PPP) for modeling the spatial distribution of the BSs. This means BSs are uniformly distributed across the entire region and the mean number of BSs per unit area is λ. The Poisson distribution is well-accepted as a spatial distribution model in a large-scale wireless network [15]. Fig. 2 shows one example of spatial distribution for outdoor environments. We assume that each BS contains at least one UE within its radius R_s and denote Π_U as the set of UEs [16], [17]. The pathloss between transmitter and receiver in the outdoor environments is then given by [18]

$$l_{out}^{(\mathrm{dB})}(d) = 140.7 + 40\log_{10}\left(d/10^3\right). \quad (3)$$

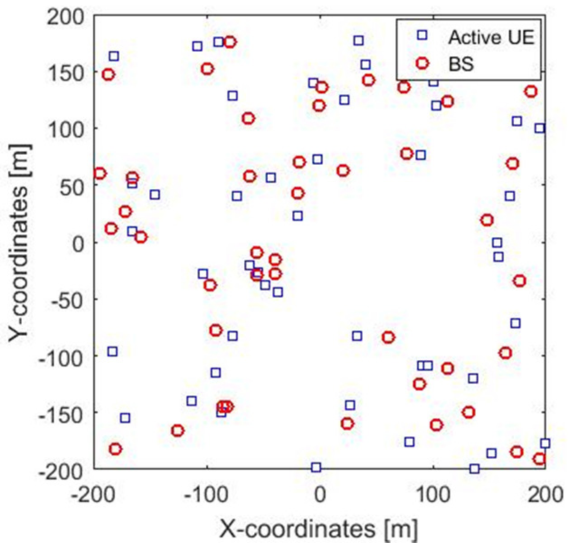

FIGURE 2. PPP-based outdoor model.

B. RECEIVED SIR

To measure the received signal to interference ratio (SIR), we arbitrarily select a typical UE and its associated BS as the UE and the BS of interest, denoted by UE_0 and BS_0, respectively. Since a UDN is generally located in an interference-limited environment [19], we assume that the noise power is negligible in this paper.

In the UDN, the received SIR of the UE_0 can be written as

$$\gamma_m^{\mathrm{DL}} = \frac{P_B \delta_0 l(d_0)}{\sum_{j\in\Pi_B} P_B \delta_j l(d_j) + 1_{\mathrm{FD}} \sum_{j\in\Pi_U} P_U \delta_j l(d_j) + \beta P_U}, \quad (4)$$

where $m \in \{\mathrm{FD}, \mathrm{HD}\}$; P_B and P_U are the transmit power of the BS and the UE, respectively; δ_i is the i.i.d. fading channel gain of the link, i.e., $\delta_i \sim \exp(1)$; $l(d)$ is the pathloss with distance d in the power scale depending on the propagation environments, such as outdoor environments, indoor environments, including the same and different buildings; d_0 is the distance between UE_0 and BS_0; d_j is the distance between the receiver of interest and the node j. 1_{FD} is a FD indicator which means when $m = \mathrm{FD}$, $1_{\mathrm{FD}} = 1$. β means the ratio of the residual SI where $\beta = 0$ denotes perfect cancellation. If $m = \mathrm{HD}$, $1_{\mathrm{FD}} = 0$ and $\beta = 0$.

Similarly, the received SIR of the BS_0 can be given as

$$\gamma_m^{\mathrm{UL}} = \frac{P_U \delta_0 l(d_0)}{\sum_{j\in\Pi_U} P_U \delta_j l(d_j) + 1_{\mathrm{FD}} \sum_{j\in\Pi_B} P_B \delta_j l(d_j) + \beta P_B}. \quad (5)$$

C. NETWORK THROUGHPUT

We use network throughput as the main metric for evaluating the performance of the UDN [4]. Network throughput is an important performance metric in UDN, because it allows us to see how the performance of the entire network varies with BS density. The network throughput can be defined as the average number of successfully transmitted bits per second per Hz per unit area, which is represented as [4]

$$\mathcal{S} = \lambda R_0 (1 - p_{out}), \quad (6)$$

where λ is the BS density, p_{out} is the outage probability, and $R_0 \triangleq \log_2(1 + \hat{\gamma})$ is the target rate with a certain SIR threshold $\hat{\gamma}$. In (6), the outage probability can be defined as

$$p_{out} = \Pr\left[\log_2(1 + \gamma) < R_0\right]. \quad (7)$$

Network throughput is actually reflected in performance only for links that satisfy quality of service (QoS) of the system. In the UDN environment where the FD system is applied, the doubled inter-cell interference leads to an increase in the number of links that do not satisfy the QoS of the system. In order to reflect this effect, it is necessary to use the network throughput as a performance metric.

III. CONVENTIONAL FD IN UDN

As mentioned earlier, the throughput gain of FD over traditional HD is significantly degraded by the increase in inter-cell interference. In this section, the performances of HD and FD are compared in terms of network throughput for outdoor scenarios.

A. NETWORK THROUGHPUTS OF CONVENTIONAL METHODS

In a UDN, the network throughput of the downlink (DL) in an HD system can be represented as

$$\mathcal{S}_{\mathrm{HD}}^{\mathrm{DL}} = \frac{\lambda}{2} R_0 \Pr\left[\log_2\left(1 + \gamma_{\mathrm{HD}}^{\mathrm{DL}}\right) \geq R_0\right]. \quad (8)$$

In this case, we have reflected the fact that the active time of the DL is half of the total time. From (8), the SIR threshold of the HD is $\hat{\gamma}_{\mathrm{HD}} = 2^{R_0} - 1$.

Theorem 1: The successful transmission probability $(1 - p_{out})$ of the DL in the HD system can be expressed as

$$\Pr\left[\gamma_{HD}^{DL} \geq \hat{\gamma}_{HD}\right] = \frac{1 - \exp\left\{-K_1(\alpha)\lambda \hat{\gamma}_{HD}^{2/\alpha} R_s^2\right\}}{K_1(\alpha)\lambda \hat{\gamma}_{HD}^{2/\alpha} R_s^2}, \quad (9)$$

where $K_1(\alpha)$ is

$$K_1(\alpha) = \frac{2\pi^2}{\alpha} \csc\left(\frac{2\pi}{\alpha}\right). \quad (10)$$

Proof: The proof is provided in Appendix A. ■

Before representing the network throughput of the uplink (UL) in the HD system, an explanation is needed regarding the distribution of the UEs. In our system model, each UE is uniformly located within small cell radius R_s. The position of the UEs is random independent displacement of the position of the BSs. The random independent displacement of a PPP forms another PPP [20]. Therefore, any analysis of the network throughput of the UL in the HD system can use the same process as that of the DL. Consequently, the result is that $\Pr\left[\gamma_{\mathrm{HD}}^{\mathrm{UL}} \geq \hat{\gamma}\right] = \Pr\left[\gamma_{\mathrm{HD}}^{\mathrm{DL}} \geq \hat{\gamma}\right]$.

Using (8) and (9), the network throughput of the HD system can be represented as

$$\mathcal{S}_{\mathrm{HD}} = \frac{\lambda}{2} R_0 \Pr\left[\gamma_{\mathrm{HD}}^{\mathrm{DL}} \geq \hat{\gamma}_{\mathrm{HD}}\right] + \frac{\lambda}{2} R_0 \Pr\left[\gamma_{\mathrm{HD}}^{\mathrm{UL}} \geq \hat{\gamma}_{\mathrm{HD}}\right]. \tag{11}$$

Now let us consider the network throughput with FD system. Many studies have recently been conducted on SI cancellation in FD systems. These results show that the SI can be removed at the noise level [21], [22]. In a UDN, noise level power can be ignored due to the nature of the interference-limited environment. In this section, therefore, we assume that the residual SI is negligible. The network throughput in an FD system can be represented as

$$\mathcal{S}_{\mathrm{FD}}^{l} = \lambda R_0 \Pr\left[\log_2\left(1 + \gamma_{\mathrm{FD}}^{l}\right) \geq R_0\right], \tag{12}$$

where $l \in \{\mathrm{DL}, \mathrm{UL}\}$. From (12), the SIR threshold of the FD is $\hat{\gamma}_{\mathrm{FD}} = 2^{R_0} - 1$.

Theorem 2: The successful transmission probability of the DL in the FD system can be expressed as

$$\Pr\left[\gamma_{FD}^{DL} \geq \hat{\gamma}_{FD}\right] = \begin{cases} \dfrac{1 - \exp\left\{-K_2(\alpha)\lambda \hat{\gamma}_{FD}^{2/\alpha} R_s^2\right\}}{K_2(\alpha)\lambda \hat{\gamma}_{FD}^{2/\alpha} R_s^2}, & \text{if } P_B = P_U, \\ \dfrac{1 - \exp\left\{-K_3(\alpha)\lambda \hat{\gamma}_{FD}^{2/\alpha} R_s^2\right\}}{K_3(\alpha)\lambda \hat{\gamma}_{FD}^{2/\alpha} R_s^2}, & \text{otherwise} \end{cases} \tag{13}$$

where $P_R = P_U/P_B$, $K_2(\alpha)$ and $K_3(\alpha)$ are

$$K_2(\alpha) = \frac{2\pi^2}{\alpha} \csc\left(\frac{2\pi}{\alpha}\right)\left(1 + \frac{2}{\alpha}\right),$$
$$K_3(\alpha) = \frac{2\pi^2}{\alpha} \csc\left(\frac{2\pi}{\alpha}\right) \frac{P_R^{2/\alpha+1} - 1}{P_R - 1}. \tag{14}$$

And the successful transmission probability of the UL in the FD system can be written as

$$\Pr\left[\gamma_{FD}^{UL} \geq \hat{\gamma}_{FD}\right] = \begin{cases} \Pr\left[\gamma_{FD}^{DL} \geq \hat{\gamma}_{FD}\right] & \text{if } P_B = P_U, \\ \dfrac{1 - \exp\left\{-K'_3(\alpha)\lambda \hat{\gamma}_{FD}^{2/\alpha} R_s^2\right\}}{K'_3(\alpha)\lambda \hat{\gamma}_{FD}^{2/\alpha} R_s^2} & \text{otherwise}, \end{cases} \tag{15}$$

where $P'_R = P_B/P_U$, $K'_3(\alpha)$ is

$$K'_3(\alpha) = \frac{2\pi^2}{\alpha} \csc\left(\frac{2\pi}{\alpha}\right) \frac{(P'_R)^{2/\alpha+1} - 1}{P'_R - 1}. \tag{16}$$

Proof: The proof is provided in Appendix B. ■

With (12), (13), and (15), the network throughput of the FD system can be represented as

$$\mathcal{S}_{\mathrm{FD}} = \lambda R_0 \Pr\left[\gamma_{\mathrm{FD}}^{\mathrm{DL}} \geq \hat{\gamma}_{\mathrm{FD}}\right] + \lambda R_0 \Pr\left[\gamma_{\mathrm{FD}}^{\mathrm{UL}} \geq \hat{\gamma}_{\mathrm{FD}}\right]. \tag{17}$$

B. SIMULATION RESULTS FOR HD AND FD IN OUTDOOR SCENARIOS

To compare conventional FD and HD, we show the simulated network throughputs for outdoor scenarios. We assume the noise floor is -104 *dBm*, the small cell radius $R_s = 30$ *m*, the transmit power of the BS and that of the UE are 26 *dB* and 23 *dB*, respectively. As mentioned before, the SI is suppressed to the noise level [21], [22]. Therefore, the ratio of the residual SI is $\beta = -130$ *dB* in our simulations.

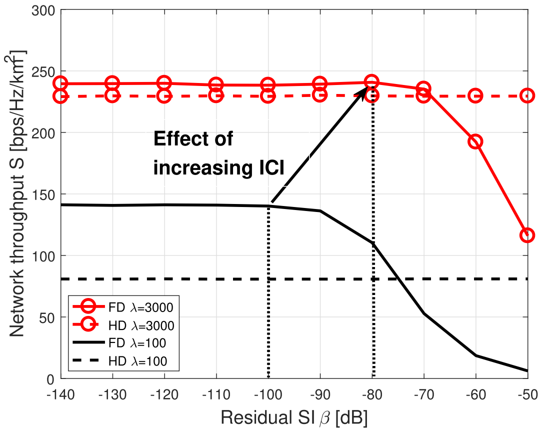

FIGURE 3. Network throughputs with FD and HD with respect to the residual SI in outdoor scenarios at $R_0 = 1$.

Fig. 3 represents the network throughputs for FD and HD according to the residual SI β in an outdoor environment with $R_0 = 1$. When λ is high enough, the inter-cell interference is significantly stronger than the SI, and the effect of the SI on performance becomes negligible. If $\lambda = 100$, the FD receiver has to suppress the SI at least -100 *dBm* to achieve the maximum network throughput. It means that if the SI is canceled by 100 *dBm*, the effect of the SI on the performance becomes negligible. When $\lambda = 3000$, the FD system can obtain maximum performance with -80 *dBm* SI cancellation. This shows that if the SI is canceled by 80 *dBm*, the impact of the SI on performance is negligible. These results confirm that the use of FD in the UDN environment is less constrained by the SIC performance than in the case of the low density environment.

Fig. 4 shows network throughputs for conventional FD and HD in an outdoor environment with $R_0 = 1$. When λ is low, the conventional FD shows better performance than the conventional HD. Under this condition, the advantage from using the full resources of the FD is more dominant compared to the degradation from interference by the FD. However, when λ increases, the gap between the HD and the FD decreases. In addition, the performance of the FD is almost the same as that of the HD at $\lambda = 3000$. Due to the simultaneous transmission and reception, FD systems suffer from inter-cell interference which is twice as strong as the inter-cell interference of HD systems. When the BS density is increased, the degradation from the doubling of the inter-cell interference becomes greater than the benefit from using

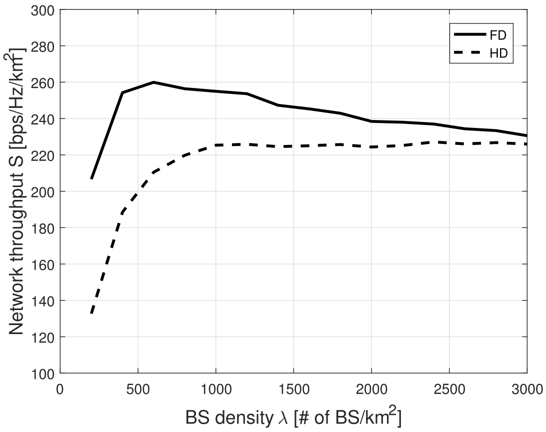

FIGURE 4. Simulated network throughputs with FD and HD in outdoor scenarios at $R_0 = 1$.

full resources with cell densification. Accordingly, we need to explore how to mitigate this problem in UDNs.

IV. RESOURCE SPLIT FD FOR UDN ENVIRONMENT

In this paper, we propose a new FD operation in order to mitigate the heavy inter-cell interference in UDNs, which was discussed in the previous section. We begin by investigating the basic idea of the proposed FD operation and its practical feasibility with theoretical analysis.

A. BASIC IDEA BEHIND RESOURCE SPLIT FD

As depicted in Fig. 5, the proposed FD operation is simple. We first divide the entire set of time and frequency resources into two resources with the same size. All BSs are spatially partitioned into two disjointed groups. In the first group, the BSs and UEs transmit and receive their data signals in the first half of the resources in a FD manner. Likewise, in the second group, the BSs and UEs perform the same operation in the second half of the resources in the FD fashion. In this way, we can considerably reduce the inter-cell interference in the UDN environment as shown in Fig. 6. Compared to the HD system, each small cell can avoid the nearest interferer with the grouping algorithm which is explained in next subsection. In this paper, we refer to this type of FD operation as **resource split (RS) FD**.

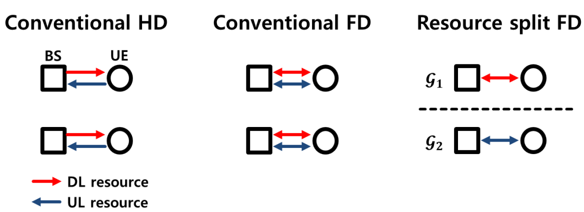

FIGURE 5. Resource assignments of conventional HD, conventional FD, and proposed resource split FD.

B. GROUPING METHODS IN THE PROPOSED RS FD

When operating with proposed RS FD, how the set of all BSs is divided into two groups is very important. Since the BSs within the same group utilize the same resources in the RS FD, a well-designed grouping method can alleviate the inter-cell interference. Let us denote ($\mathcal{G}_1$) and ($\mathcal{G}_2$) as the first and second group utilizing the first half and second half of the resources, respectively. In this paper, we will consider two grouping methods: random grouping and sequential grouping.

- Random grouping: Random grouping is where each BS randomly selects its group from among group1 ($\mathcal{G}_1$) and group2 ($\mathcal{G}_2$) with the same probability. With this method, the BSs can simply divide into groups without any complicated additional process. Random grouping also operates in a decentralized way. Therefore, there is no need to exchange signals containing group information.
- Sequential grouping: Sequential grouping is based on knowing the location information for the UDN BSs. In our system model, the macro BSs coexist with UDN BSs and share the location information of the UDN BSs. When an arbitrary UDN BS is set as a reference BS, the reference BS is defined as the first BS. The macro BS searches for the UDN BS closest to the reference BS. This closest BS is defined as the second BS. Among the non-selected BSs, the macro BS finds the nearest BS to the second BS, and selects it as the third BS. By repeating this process, we can arrange all of the BSs in order. The BSs are then divided into two groups which are $\mathcal{G}_1$, containing odd-ordered BSs, and $\mathcal{G}_2$, containing even-ordered BSs.

The sequential grouping is summarized in Algorithm 1. We define the number of UDN BSs in our system as N, set of ungrouped BSs as $\mathcal{G}_0$, and the distance between BS_i and BS_j as d_{ij}.

Algorithm 1 Sequential Grouping Algorithm

Input: $\mathcal{G}_0 = \{\mathbf{BS}_1, \mathbf{BS}_2, \cdots, \mathbf{BS}_N\}$
Initialize:
  $i = 1, n = 1,$
  $\mathcal{G}_0 \leftarrow \mathcal{G}_0 - \{\text{BS}_1\}, \mathcal{G}_1 \leftarrow \mathcal{G}_1 \bigcup \{\text{BS}_1\}.$
for t = 2 to N **do**
  $j^* = \arg\min_j d_{ij}$ subject to $\text{BS}_j \in \mathcal{G}_0$;
  $\mathcal{G}_0 \leftarrow \mathcal{G}_0 - \{\text{BS}_j\}$;
  if n is odd **then**
    $\mathcal{G}_1 \leftarrow \mathcal{G}_1 \bigcup \{\text{BS}_j\}$;
  else
    $\mathcal{G}_2 \leftarrow \mathcal{G}_2 \bigcup \{\text{BS}_j\}$;
  $i \leftarrow j$;
  end
end
Output: $\mathcal{G}_1, \mathcal{G}_2$

C. LOCATION INFORMATION OF SMALL CELL BSS

For the sequential grouping, the proposed approach requires the core network to know the locations of the small cell BSs. It is important to describe how accurate location information is obtained for all the BSs under consideration. For that

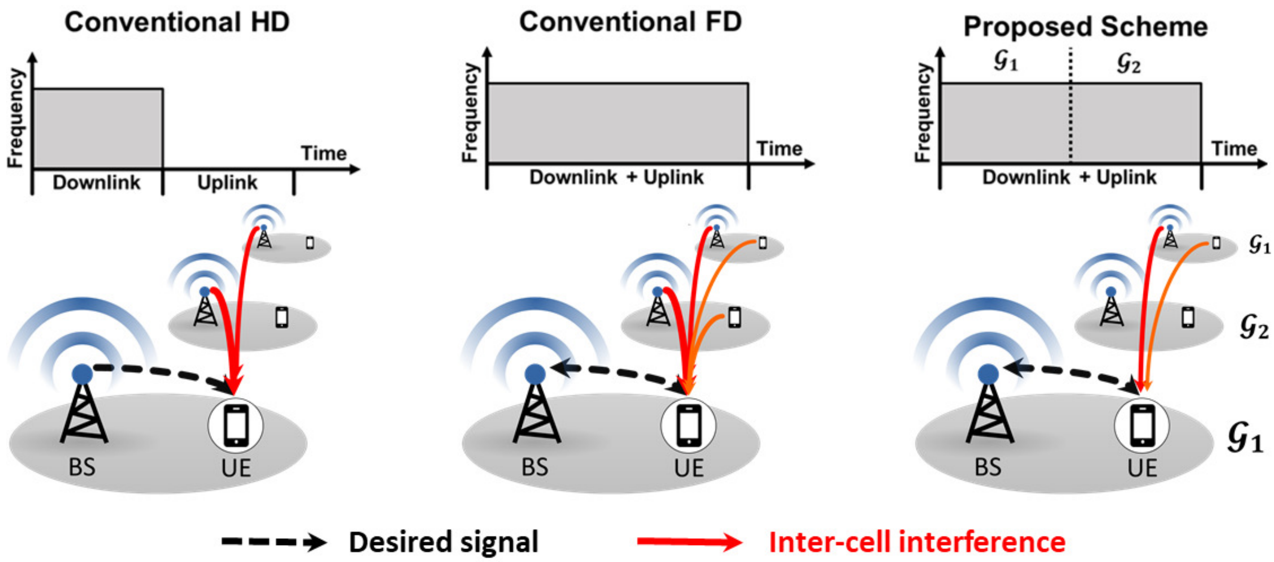

FIGURE 6. Examples of interference patterns with respect to different schemes.

purpose, we will introduce a few methods here that can be used to collect femto cell location information [23].

The simplest of these is using the global positioning system (GPS). Some femto cells have GPS or assisted-GPS capabilities. These types of BSs can provide more accurate location information to the operators.

The operator can also use IP addresses to find the locations of femto cells. Specifically, many broadband access providers assign their pool of public IP addresses based on the geographic locations of the users, and the user's IP address remains relatively static for a long period of time. The core networks of operators can then query the network database to obtain the port number bound with the IP address, and then determine the location of the femto cell.

Another approach relies on the assistance of other BSs in the neighborhood whose locations are known to the core networks. When a femto cell BS is turned on, it scans for neighboring information such as cell ID, PLMN ID, and other information. If the femto cell can collect this information from more than three neighbors and report it, operators can determine the locations of the femto cells using triangulation method.

D. NETWORK THROUGHPUT OF RS FD

When the proposed method is used, the network throughput in an RS FD system can be represented as

$$\mathcal{S}_{\mathrm{PR}}^{l} = \frac{\lambda}{2} R_0 \Pr\left[\log_2\left(1+\gamma_{\mathrm{PR}}^{l}\right) \geq R_0\right], \tag{18}$$

where $l \in \{\mathrm{DL}, \mathrm{UL}\}$. From (18), the SIR threshold for RS FD is $\hat{\gamma}_{\mathrm{PR}} = 2^{R_0} - 1$.

As described previous subsections, when the proposed scheme operates, all BSs are divided into two groups. Therefore, UL and DL of group1 ($\mathcal{G}_1$) and group2 ($\mathcal{G}_2$) with density of $\lambda/2$ are transmitted simultaneously. When the proposed RS FD with the random grouping algorithm is used, the successful transmission probability is easily obtained by replacing λ with $\lambda/2$ in the successful transmission probability of the conventional FD system. If $P_B = P_U$, the successful transmission probability of the RS FD system with the random grouping algorithm can be written as

$$\Pr\left[\gamma_{\mathrm{PR}}^{\mathrm{DL}} \geq \hat{\gamma}_{\mathrm{PR}}\right] = \Pr\left[\gamma_{\mathrm{PR}}^{\mathrm{UL}} \geq \hat{\gamma}_{\mathrm{PR}}\right] = \frac{1-\exp\left\{-K_2(\alpha)\frac{\lambda}{2}\hat{\gamma}_{\mathrm{PR}}^{2/\alpha}R_s^2\right\}}{K_2(\alpha)\frac{\lambda}{2}\hat{\gamma}_{\mathrm{PR}}^{2/\alpha}R_s^2}. \tag{19}$$

When $P_B \neq P_U$, the successful transmission probability of the RS FD system with the random grouping algorithm can be written as

$$\Pr\left[\gamma_{\mathrm{PR}}^{\mathrm{DL}} \geq \hat{\gamma}_{\mathrm{PR}}\right] = \frac{1-\exp\left\{-K_3(\alpha)\frac{\lambda}{2}\hat{\gamma}_{\mathrm{PR}}^{2/\alpha}R_s^2\right\}}{K_3(\alpha)\frac{\lambda}{2}\hat{\gamma}_{\mathrm{PR}}^{2/\alpha}R_s^2},$$
$$\Pr\left[\gamma_{\mathrm{PR}}^{\mathrm{UL}} \geq \hat{\gamma}_{\mathrm{PR}}\right] = \frac{1-\exp\left\{-K'_3(\alpha)\frac{\lambda}{2}\hat{\gamma}_{\mathrm{PR}}^{2/\alpha}R_s^2\right\}}{K'_3(\alpha)\frac{\lambda}{2}\hat{\gamma}_{\mathrm{PR}}^{2/\alpha}R_s^2}. \tag{20}$$

With (18), (19), and (20), the network throughput in the RS FD system can be represented as

$$\mathcal{S}_{\mathrm{PR}} = \frac{\lambda}{2} R_0 \Pr\left[\gamma_{\mathrm{PR}}^{\mathrm{DL}} \geq \hat{\gamma}_{\mathrm{PR}}\right] + \frac{\lambda}{2} R_0 \Pr\left[\gamma_{\mathrm{PR}}^{\mathrm{UL}} \geq \hat{\gamma}_{\mathrm{PR}}\right]. \tag{21}$$

Using (13) and (20), we compare the network throughput of the conventional FD system and that of the RS FD system with the sequential grouping algorithm. In the case of the proposed sequential scheme, we derived the lower bound for the performance comparison. When the RS FD system with the sequential grouping algorithm is applied, each BS chooses the resource which is not selected by the nearest BS. As a result, the strongest interference among the interferences received when using the conventional FD can be avoided. If we assume that the node of conventional FD system receives interference from N cells, the proposed scheme will receive interference from $N/2$ cells in the same setup. The total interference generated from $N-1$ cells excluding the nearest cell among the N cells in conventional FD system is used as lower bound of the RS FD system with the sequential grouping algorithm.

Then, the lower bound for the SIR of the RS FD system with the sequential grouping algorithm can be written as

$$\gamma_{\mathrm{PR}}^{\mathrm{DL}} > \frac{P_B \delta_0 d_0^{-\alpha}}{I_{\mathrm{FD}} - I_1}, \tag{22}$$

where I_1 is the interference from the nearest cell. We define k as $k = I_1 / I_{\mathrm{FD}}$ and the lower bound for the successful transmission probability of the RS FD system with the sequential grouping algorithm is represented as

$$\begin{aligned} &\Pr\left[\gamma_{\mathrm{PR}}^{\mathrm{DL}} \geq \hat{\gamma}_{\mathrm{PR}}\right] \\ &\quad > \Pr\left[P_B\delta_0 \geq \hat{\gamma}_{\mathrm{PR}} d_0^{\alpha}(1-k)\, I_{\mathrm{FD}}\right] \\ &\quad = \int_0^{\infty} \Pr\left[P_B\delta_0 \geq \hat{\gamma}_{\mathrm{PR}} d_0^{\alpha}\,(1-k)\, I\right] f_{I_{\mathrm{FD}}}(I)\, dI \\ &\quad = \mathcal{L}_{I_{\mathrm{FD}}}\left((1-k)\,\hat{\gamma}_{\mathrm{PR}} d_0^{\alpha} / P_B\right). \end{aligned} \tag{23}$$

And the lower bound for the network throughput of the RS FD system with the sequential grouping algorithm can be expressed as

$$\begin{aligned} \mathcal{S}_{\mathrm{PR}}^{\mathrm{DL}} > \mathcal{S}_{\mathrm{PR,LB}}^{\mathrm{DL}} &= \frac{\lambda}{2} R_0 \mathcal{L}_{I_{\mathrm{FD}}}\left((1-k)\,\hat{\gamma}_{\mathrm{PR}} d_0^{\alpha} / P_B\right) \\ &= \frac{\lambda}{2} R_0 \frac{1 - \exp\left\{-K_3(\alpha)\,\lambda (1-k)^{2/\alpha} \hat{\gamma}_{\mathrm{PR}}^{2/\alpha} R_s^2\right\}}{K_3(\alpha)\,\lambda(1-k)^{2/\alpha}\hat{\gamma}_{\mathrm{PR}}^{2/\alpha} R_s^2}. \end{aligned} \tag{24}$$

With $\hat{\gamma}_{\mathrm{FD}} = \hat{\gamma}_{\mathrm{PR}} = 2^{R_0} - 1$, (12), and (24), after some algebraic manipulation, $\mathcal{S}_{\mathrm{PR}}^{\mathrm{DL}} > \mathcal{S}_{\mathrm{PR,LB}}^{\mathrm{DL}} > \mathcal{S}_{\mathrm{FD}}^{\mathrm{DL}}$ is equivalently converted into

$$\mathcal{S}_{\mathrm{PR,LB}}^{\mathrm{DL}} > \mathcal{S}_{\mathrm{FD}}^{\mathrm{DL}} \Leftrightarrow \lambda > \frac{1}{A} \ln \frac{2(1-k)^{2/\alpha} - 1}{2(1-k)^{2/\alpha} - \exp\left((1-k)^{2/\alpha}\right)}, \tag{25}$$

where $A = K_3(\alpha)\,\hat{\gamma}^{2/\alpha} R_s^2$. The UL case can also be derived in the same way as the DL case shown above. From (25), we can say that the network throughput of the RS FD system with the sequential grouping algorithm is better than that of the conventional FD for a sufficiently large λ satisfying the above conditions.

V. NUMERICAL RESULTS

As mentioned above, we considered two simulation scenarios in UDN: outdoor environment and indoor environment. For outdoor scenario, we exploited PPP framework for BS deployment, which has been popularly used for modeling small cell network [7], [16], [17], [19], [24]. For indoor scenario, we utilized dual-stripe apartment block model for dense urban city, which was certified by 3GPP standard [5], [14]. Range of the BS densities was widely considered from 200 to 3000. Table 1 summarizes the system parameters.

TABLE 1. System parameters.

	Parameters	Values	Parameters	Values
Common parameters	BS density λ	200~3000 [#/km^2]	Noise floor	-104 [dBm]
	BS transmit power P_B	26 [dBm]	UE transmit power P_U	23 [dBm]
	Residual self Interference β	-130 [dB]		
	Parameters	**Values**		
Indoor-specific parameters	Building deployment	Dual-stripe urban model, random number of floors uniform between 2 and 5, 10 rooms for each stripe (10m×10m for 1 room), apartment block density λ_B=50 [#/ km^2]		
	Cell deployment	BSs are uniformly dropped inside the deployed buildings		
	UE deployment	Each BS has at least one UE within the same apartment		
	Small-scale fading	Rician fading channel with K=15dB for the same room, Rayleigh fading channel for the different room or building		
	Pathloss model	In the same building, $l_{in,s}^{(dB)}(d) = 43.26 + 20\log_{10}(10d) + 0.5\chi + q_{iw}L_{iw}$ In the different building, $l_{in,d}^{(dB)}(d) = \max(20.1 + 37.6\log_{10}(10d),\ 43.26 + 20\log_{10}(10d)) + 0.5\chi + q_{iw}L_{iw} + q_{ow}L_{ow}$ q_{iw}: # of inner walls, q_{ow}: # of outer walls, χ : random variable following uniform distribution U(0,25), L_{iw} = 5 dB: penetration loss of inner wall, L_{ow} = 23 dB: penetration loss of outer wall		
Outdoor-specific parameters	Cell deployment	PPP modeling, BSs are uniformly distributed over 2-dimensional plane		
	UE deployment	Each BS has at least one UE within its radius $R_s = 30m$		
	Small-scale fading	Rayleigh fading channel		
	Pathloss model	$l_{out}^{(dB)}(d) = 140.7 + 40\log_{10}(d/10^3)$		

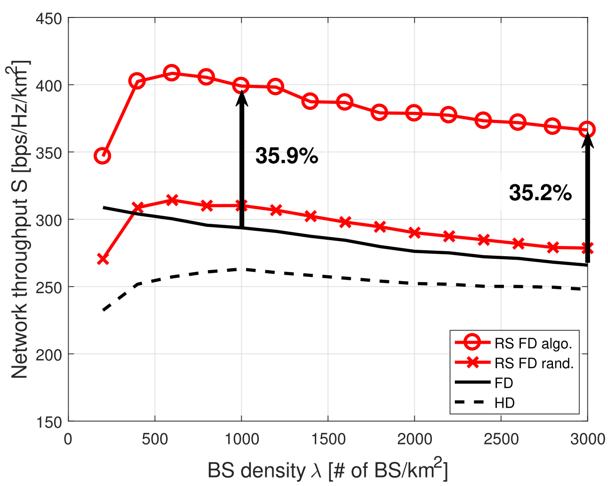

FIGURE 7. Comparison of network throughput and BS density for the outdoor scenario at $R_0 = 3$.

Fig. 7 shows the network throughput performances with respect to the BS density λ in an outdoor environment with $R_0 = 3$. When the BS density increases, the performance gain of conventional FD over HD is degraded by the increase in inter-cell interference. Our proposed schemes can overcome this limitation. The proposed RS FD with the sequential grouping algorithm shows better performance than the conventional FD by about 35.9% and 35.2% at $\lambda = 1000, 3000$, respectively. The performance gain of the proposed scheme derives from the fact that the inter-cell interference is reduced given that the number of BSs sharing resources is decreased by half, and that the sequential grouping algorithm is able to avoid the most severe interference. When the sequential grouping algorithm is applied, each BS and its nearest BS are arranged to different groups and it is possible to avoid the strongest interference from the nearest BS. With the random grouping algorithm, there is 50% chance of assigning a BS and its nearest BS to the same group. According to the simulation results, the power of interference from the nearest BS is about 63% of the power of total inter-cell interference and it has a significant impact on system performance. Therefore, the sequential grouping algorithm can obtain better performance than the random grouping algorithm.

Fig. 8 illustrates the network throughput performances with respect to the BS density λ in an indoor environment with $R_0 = 5$. When the BS density is low, the conventional FD shows better performance compared to HD. The inner and outer walls weaken the effect of the inter-cell interference in the indoor scenario compared to the outdoor scenario. Similar to the result of the outdoor case, the gap between the conventional FD and the HD closes as the BS density increases. When $\lambda < 1000$, the network throughput of the conventional FD is better than the network throughputs of the proposed schemes. The performance gain of the proposed scheme comes from the reduction in inter-cell interference. In this experimental environment, the effect of inter-cell interference is small. Therefore, the gain of the proposed scheme becomes smaller than in Fig. 7. When $\lambda > 1000$, the proposed RS FD with sequential grouping algorithm shows better performance than the conventional FD. The proposed RS FD with sequential grouping algorithm shows better performance than the conventional FD by about 63.4% at $\lambda = 3000$.

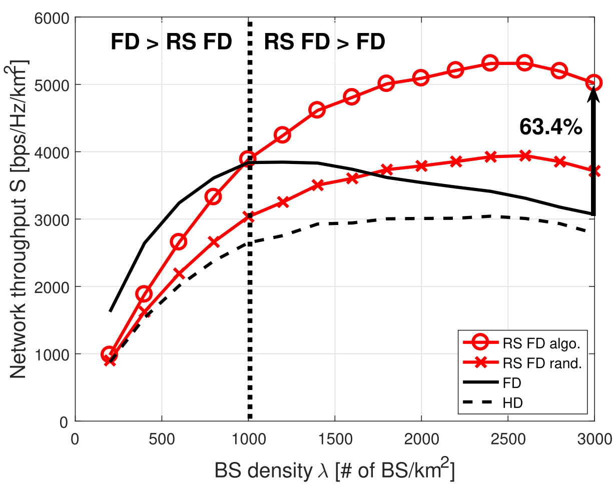

FIGURE 8. Comparison of network throughput and BS density for the indoor scenario at $R_0 = 5$.

Fig. 9 shows the network throughput performances under an asymmetric traffic model in an outdoor environment when $R_0 = 1$ and $\lambda = 1000$. In this simulation, μ stands for the

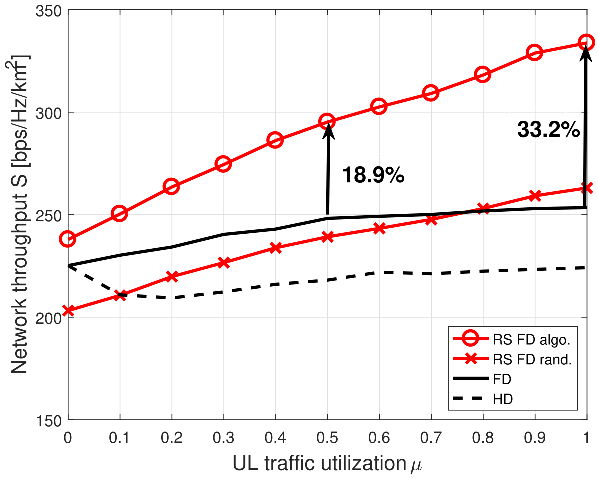

FIGURE 9. Network throughput for asymmetric traffic model in the outdoor environment, when $R_0 = 1$ and $\lambda = 1000$.

UL traffic utilization probability. In this asymmetric traffic model, we assume that the DL always has data to send and the UL has data to transmit probabilistically. UL traffic utilization is defined as the probability of having UL data to transmit. Also, we consider that the HD uses UL and DL resources divided by the ratio of the probability of traffic. When there is no UL traffic, the DL of the HD uses all the time resources because there is no UL transmission data, and in this case the HD and the conventional FD show the same performance. Conventional FD and HD have small increases in performance as traffic increases. This is because the performance gain from UL activation is almost the same as the performance loss caused by the new inter-cell interference. Unlike the conventional schemes, the performance of the proposed schemes increases steadily as UL traffic increases. The proposed RS FD with the sequential grouping algorithm shows better performance than the conventional FD by about 18.9% and 33.2% at $\mu = 0.5, 1$, respectively. From this result, we can see that the proposed scheme is robust against inter-cell interference.

Fig. 10 (a) illustrates the network throughput performances according to the target rate R_0 in an outdoor environment with $\lambda = 1000$. The overall tendency is that when R_0 is low, the network throughput also increases as R_0 increases. This is because, from (6), the performance gain from increasing R_0 is larger than the performance loss due to the increasing outage probability. When R_0 increases, $\hat{\gamma} = 2^{R_0} - 1$ also increases, and is related to the outage probability. When R_0 increases beyond a certain value, the network throughput decreases as R_0 increases. In this case, the performance loss from the increasing outage probability is larger than the performance gain from the increasing R_0. This is because $\hat{\gamma}$ increases exponentially as R_0 increases. Comparing the conventional FD with the HD, the network throughput gain achieved by using conventional FD decreases as R_0 increases. And the RS FD with sequential grouping algorithm shows a roughly 36.5% and 41.4% better performance than conventional FD with $R_0 = 5, 10$, respectively.

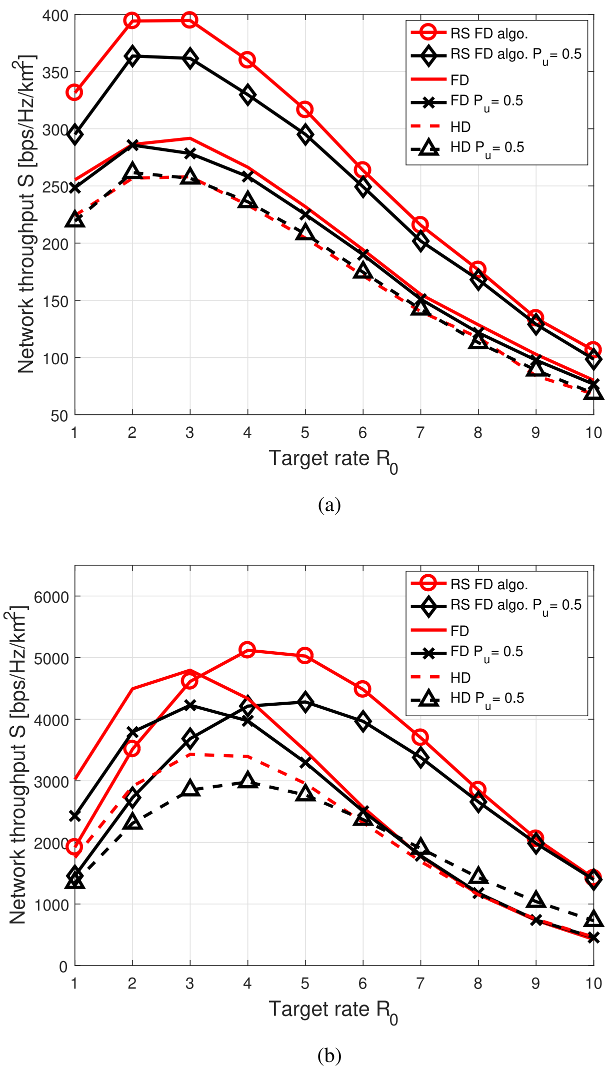

FIGURE 10. Network throughput versus the target rate. (a) Outdoor environment. (b) Indoor environment.

With the asymmetric traffic model, the conventional FD and the HD show almost the same performance. Conversely, the proposed scheme shows a performance loss when R_0 is small, and the performance loss tends to decrease as R_0 increases. When the UL traffic decreases, the number of UL transmissions decreases, producing two effects. The performance is reduced by the number of ULs that are turned off, and increases as the inter-cell interference is reduced. With the conventional FD and the HD, the impact of the performance degradation is almost the same as the impact of the performance increase. With the proposed scheme, the impact of the performance degradation is greater than the impact of the performance increase.

Fig. 10 (b) demonstrates the network throughput performances according to the target rate R_0 in an indoor environment with $\lambda = 2000$. Compared to the outdoor scenario, the value of the target rate which shows the best performance is shifted to the right. In detail, the best performance of the conventional FD and the HD appear when $R_0 = 3$, and that for the RS FD appears when $R_0 = 4$. The reason for these results is that as the intensity of the inter-cell interference is weakened due to the walls, the SINR improves and it is possible to satisfy the higher target rate. Furthermore, as the target rate increases, the performance of the conventional FD and the HD becomes more and more similar. Unlike the outdoor environment, the conventional FD shows the best performance in the indoor environment where $R_0 \leq 3$. This is because the SINR of conventional FD is made good enough by decreasing the inter-cell interference, enabling the conventional FD to use its full set of resources. This fact makes it possible to determine which scheme is best to use when the BS density and the target rate are set as system parameters. The RS FD with proposed algorithm delivers 44.1% and 233.0% better performance than conventional FD with $R_0 = 5$, 10, respectively.

Thanks to the inter-cell interference reduction effect due to the walls, the performance of the conventional FD and the RS FD are degraded under the asymmetric traffic model. In the HD case, when $R_0 \geq 6$, performance improves with the asymmetric traffic model. This is because the performance loss caused by the number of ULs that are turned off is smaller than the performance gain due to the inter-cell interference reduction.

VI. CONCLUSIONS

In this paper, we investigated a way forward to improve the network throughput, when FD is employed in UDN environment. Specifically, we first identified that the performance gain of FD over HD is significantly reduced with cell densification. Our proposed a new FD operation, called RS FD, can effectively alleviate the heavy inter-cell interference caused by FD use. The basic idea behind the proposed RS FD is to divide the set of small cells into two groups, with each group using half of the available resources. In UDN environment, the proposed RS FD outperforms the conventional FD and HD in both outdoor and indoor scenarios. On the basis of this paper, there will be several research topics as follows: performance analysis of RS FD, combination with advanced power control method, and consideration of multiple antennas.

APPENDIX A
PROOF OF THEOREM 1

In the HD system, the received SIR of the UE_0 can be written as

$$\gamma_{\mathrm{HD}}^{\mathrm{DL}} = \frac{P_B \delta_0 l\left(d_0\right)}{\sum\limits_{j \in \Pi_B} P_B \delta_j l\left(d_j\right)} \approx \frac{P_B \delta_0 d_0^{-\alpha}}{I_{\mathrm{HD}}}, \tag{26}$$

where α is the pathloss exponent and I_{HD} is the aggregate interference of the HD system. The aggregate interference of the HD system can be presented as

$$I_{\mathrm{HD}} = \sum_{j \in \Pi_B} P_B \delta_j d_j^{-\alpha}. \tag{27}$$

Then, the successful transmission probability $(1 - p_{out})$ of the DL in the HD system is given by [24].

$$\begin{aligned}\Pr\left[\gamma_{\mathrm{HD}}^{\mathrm{DL}} \geq \hat{\gamma}_{\mathrm{HD}}\right] &= \Pr\left[P_B\delta_0 \geq \hat{\gamma}_{\mathrm{HD}} d_0^{\alpha} I_{\mathrm{HD}}\right] \\ &= \int_0^{\infty} \Pr\left[P_B\delta_0 \geq \hat{\gamma}_{\mathrm{HD}} d_0^{\alpha} I\right] f_{I_{\mathrm{HD}}}(I)\, dI \\ &= \mathcal{L}_{I_{\mathrm{HD}}}\left(\hat{\gamma}_{\mathrm{HD}} d_0^{\alpha}/P_B\right), \end{aligned} \tag{28}$$

where $\mathcal{L}_{I_k}(s)$ is a Laplace transform of the probability distribution function (PDF) of I_k. $\mathcal{L}_{I_{\mathrm{HD}}}(s), \forall s > 0$ can be represented as [25].

$$\begin{aligned}\mathcal{L}_{I_{\mathrm{HD}}}(s) &= \exp\left\{-2\pi\lambda \int_0^{\infty} x E_{\delta_i}\left\{1 - e^{-sP_B\delta_i x^{\alpha}}\right\} dx\right\} \\ &= \exp\left\{-2\pi\lambda \int_0^{\infty} \frac{x}{1 + \left(s^{-1}P_B^{-1}x^{\alpha}\right)} dx\right\} \\ &= \exp\left\{-2\pi\lambda \frac{\pi \csc\left(2\pi/\alpha\right)\left(sP_B\right)^{2/\alpha}}{\alpha}\right\}. \end{aligned} \tag{29}$$

Therefore, by using (28) and (29), we can obtain

$$\begin{aligned}\Pr\left[\gamma_{\mathrm{HD}}^{\mathrm{DL}} \geq \hat{\gamma}_{\mathrm{HD}}\right] &= \exp\left\{\frac{-2\pi^2}{\alpha} \csc\left(\frac{2\pi}{\alpha}\right) \lambda \left(\hat{\gamma}_{\mathrm{HD}} d_0^{\alpha}\right)^{2/\alpha}\right\} \\ &= \exp\left\{-K_1(\alpha)\lambda d_0^2 \hat{\gamma}_{\mathrm{HD}}^{2/\alpha}\right\} \\ &= \int_0^{R_s} \exp\left\{-K_1(\alpha)\lambda \hat{\gamma}_{\mathrm{HD}}^{2/\alpha} l^2\right\} \frac{2l}{R_s^2} dl \\ &= \frac{1 - \exp\left\{-K_1(\alpha)\lambda \hat{\gamma}_{\mathrm{HD}}^{2/\alpha} R_s^2\right\}}{K_1(\alpha)\lambda \hat{\gamma}_{\mathrm{HD}}^{2/\alpha} R_s^2}, \end{aligned} \tag{30}$$

where $K_1(\alpha)$ is

$$K_1(\alpha) = \frac{2\pi^2}{\alpha} \csc\left(\frac{2\pi}{\alpha}\right). \tag{31}$$

APPENDIX B
PROOF OF THEOREM 2

In the FD system, the received SIR of the UE_0 can be written as

$$\begin{aligned}\gamma_{\mathrm{FD}}^{\mathrm{DL}} &= \frac{P_B\delta_0 l(d_0)}{\sum_{j\in\Pi_B} P_B\delta_j l(d_j) + \sum_{j\in\Pi_U} P_U\delta_j l(d_j) + \beta P_U} \\ &\approx \frac{P_B\delta_0 d_0^{-\alpha}}{I_{\mathrm{FD}}}, \end{aligned} \tag{32}$$

where I_{FD} is the aggregate interference of the FD system. The aggregate interference of the FD system can be presented as

$$I_{\mathrm{FD}} = \sum_{j\in\Pi_B} P_B\delta_j d_j^{-\alpha} + \sum_{j\in\Pi_U} P_U\delta_j d_j^{-\alpha}. \tag{33}$$

Then, $\mathcal{L}_{I_{\mathrm{FD}}}(s), \forall s > 0$ can be represented as [25]

$$\begin{aligned}\mathcal{L}_{I_{\mathrm{FD}}}(s) &= \exp\left\{-\frac{2\pi}{\alpha}\lambda E_{G_i}\left\{\int_0^{\infty} y^{2/\alpha - 1}\left(1 - e^{-sG_i/y}\right) dy\right\}\right\} \\ &= \exp\left\{-\frac{2\pi}{\alpha}\lambda E_{G_i}\left\{-(sG_i)^{2/\alpha}\Gamma\left(-\frac{2}{\alpha}\right)\right\}\right\} \\ &= \exp\left\{\frac{2\pi}{\alpha}\lambda\Gamma\left(-\frac{2}{\alpha}\right) E_{G_i}\left\{G_i^{2/\alpha}\right\} s^{2/\alpha}\right\}, \end{aligned} \tag{34}$$

where $\Gamma(x)$ is Gamma function $\Gamma(x) = \int_0^{\infty} t^{x-1}e^{-t}dt$ and $G_i = P_B\delta_{\mathrm{BSi}} + P_U\delta_{\mathrm{UEi}}$. If $P_B = P_U$, $E_{G_i}\left\{G_i^{2/\alpha}\right\}$ can be written as

$$E_{G_i}\left\{G_i^{2/\alpha}\right\} = P_B^{2/\alpha}\Gamma\left(2 + 2/\alpha\right). \tag{35}$$

In this case, the successful transmission probability of the DL in the FD system is represented as

$$\begin{aligned}&\Pr\left[\gamma_{\mathrm{FD}}^{\mathrm{DL}} \geq \hat{\gamma}_{\mathrm{FD}}\right] \\ &= \mathcal{L}_{I_{\mathrm{FD}}}\left(\hat{\gamma}_{\mathrm{FD}} d_0^{\alpha}/P_B\right) \\ &= \exp\left\{\frac{2\pi}{\alpha}\Gamma\left(-\frac{2}{\alpha}\right)\Gamma\left(2 + \frac{2}{\alpha}\right)\lambda d_0^2 \hat{\gamma}_{\mathrm{FD}}^{2/\alpha}\right\} \\ &= \exp\left\{\frac{-2\pi^2}{\alpha}\csc\left(\frac{2\pi}{\alpha}\right)\left(1 + \frac{2}{\alpha}\right)\lambda d_0^2 \hat{\gamma}_{\mathrm{FD}}^{2/\alpha}\right\} \\ &= \exp\left\{-K_2(\alpha)\lambda d_0^2 \hat{\gamma}_{\mathrm{FD}}^{2/\alpha}\right\} \\ &= \frac{1 - \exp\left\{-K_2(\alpha)\lambda \hat{\gamma}_{\mathrm{FD}}^{2/\alpha} R_s^2\right\}}{K_2(\alpha)\lambda \hat{\gamma}_{\mathrm{FD}}^{2/\alpha} R_s^2}, \end{aligned} \tag{36}$$

where $K_2(\alpha)$ is

$$K_2(\alpha) = \frac{2\pi^2}{\alpha}\csc\left(\frac{2\pi}{\alpha}\right)\left(1 + \frac{2}{\alpha}\right). \tag{37}$$

When $P_B \neq P_U$, $E_{G_i}\left\{G_i^{2/\alpha}\right\}$ can be written as

$$E_{G_i}\left\{G_i^{2/\alpha}\right\} = \frac{\Gamma\left(1 + 2/\alpha\right)\left(P_U^{2/\alpha+1} - P_B^{2/\alpha+1}\right)}{P_U - P_B}. \tag{38}$$

In this case, the successful transmission probability of the DL in the FD system is represented as

$$\begin{aligned}&\Pr\left[\gamma_{\mathrm{FD}}^{\mathrm{DL}} \geq \hat{\gamma}_{\mathrm{FD}}\right] \\ &= \mathcal{L}_{I_{\mathrm{FD}}}\left(\hat{\gamma}_{\mathrm{FD}} d_0^{\alpha}/P_B\right) \\ &= \exp\left\{\frac{2\pi}{\alpha}\Gamma\left(-\frac{2}{\alpha}\right)\Gamma\left(1 + \frac{2}{\alpha}\right)\frac{P_R^{2/\alpha+1} - 1}{P_R - 1}\lambda d_0^2 \hat{\gamma}_{FD}^{2/\alpha}\right\} \\ &= \exp\left\{-\frac{2\pi^2}{\alpha}\csc\left(\frac{2\pi}{\alpha}\right)\frac{P_R^{2/\alpha+1} - 1}{P_R - 1}\lambda d_0^2 \hat{\gamma}_{FD}^{2/\alpha}\right\} \\ &= \exp\left\{-K_3(\alpha)\lambda d_0^2 \hat{\gamma}_{\mathrm{FD}}^{2/\alpha}\right\} \\ &= \frac{1 - \exp\left\{-K_3(\alpha)\lambda \hat{\gamma}_{\mathrm{FD}}^{2/\alpha} R_s^2\right\}}{K_3(\alpha)\lambda \hat{\gamma}_{\mathrm{FD}}^{2/\alpha} R_s^2}, \end{aligned} \tag{39}$$

where $P_R = P_U/P_B$, $K_3(\alpha)$ is

$$K_3(\alpha) = \frac{2\pi^2}{\alpha}\csc\left(\frac{2\pi}{\alpha}\right)\frac{P_R^{2/\alpha+1}-1}{P_R-1}. \tag{40}$$

With (36) and (39), the successful transmission probability of the UL in the FD system can be written as

$$\Pr\left[\gamma_{\mathrm{FD}}^{\mathrm{UL}} \geq \hat{\gamma}_{\mathrm{FD}}\right] = \begin{cases} \Pr\left[\gamma_{\mathrm{FD}}^{\mathrm{DL}} \geq \hat{\gamma}_{\mathrm{FD}}\right] & \text{if } P_B = P_U, \\ \dfrac{1-\exp\left\{-K'_3(\alpha)\lambda\hat{\gamma}_{\mathrm{FD}}^{2/\alpha}R_s^2\right\}}{K'_3(\alpha)\lambda\hat{\gamma}_{\mathrm{FD}}^{2/\alpha}R_s^2} & \text{otherwise}, \end{cases} \tag{41}$$

where $P'_R = P_B/P_U$, $K'_3(\alpha)$ is

$$K'_3(\alpha) = \frac{2\pi^2}{\alpha}\csc\left(\frac{2\pi}{\alpha}\right)\frac{(P'_R)^{2/\alpha+1}-1}{P'_R-1}. \tag{42}$$

REFERENCES

[1] D. Kim, H. Lee, and D. Hong, "A survey of in-band full-duplex transmission: From the perspective of PHY and MAC layers," *IEEE Commun. Surveys Tuts.*, vol. 17, no. 4, pp. 2017–2046, Feb. 2015.

[2] A. Sabharwal, P. Schniter, D. Guo, D. W. Bliss, S. Rangarajan, and R. Wichman, "In-band full-duplex wireless: Challenges and opportunities," *IEEE J. Sel. Areas Commun.*, vol. 32, no. 9, pp. 1637–1652, Sep. 2014.

[3] H. Ju, X. Shang, H. V. Poor, and D. Hong, "Bi-directional use of spatial resources and effects of spatial correlation," *IEEE Trans. Wireless Commun.*, vol. 10, no. 10, pp. 3368–3379, Oct. 2011.

[4] M. Kamel, W. Hamouda, and A. Youssef, "Ultra-dense networks: A survey," *IEEE Commun. Surveys Tuts.*, vol. 18, no. 4, pp. 2522–2545, 4th Quart., 2016.

[5] *Small Cells and UltraSON*, San Diego, CA, USA, Qualcomm, 2014.

[6] *Small Cells, Big Opportunities*, Huawei, Shenzhen, China, Feb. 2014.

[7] Y. Park, J. Heo, and D. Hong, "Spectral efficiency analysis of ultra-dense small cell networks with heterogeneous channel estimation capabilities," *IEEE Commun. Lett.*, vol. 21, no. 8, pp. 1839–1842, Aug. 2017.

[8] W. Zhou and K. Srinivasan, "SIM+: A simulator for full duplex communications," in *Proc. Int. Conf. Signal Process. Commun. (SPCOM)*, Jul. 2014, pp. 1–6.

[9] N. H. Mahmood, G. Berardinelli, F. M. L. Tavares, and P. Mogensen, "On the potential of full duplex communication in 5G small cell networks," in *Proc. IEEE 81st Veh. Technol. Conf. (VTC Spring)*, May 2015, pp. 1–5.

[10] M. G. Sarret, G. Berardinelli, N. H. Mahmood, and P. Mogensen, "Can full duplex boost throughput and delay of 5G ultra-dense small cell networks?" in *Proc. IEEE 83rd Veh. Technol. Conf. (VTC Spring)*, May 2016, pp. 1–5.

[11] G. Berardinelli, D. A. Wassie, N. H. Mahmood, M. G. Sarret, T. B. Sorensen, and P. Mogensen, "Evaluating full duplex potential in dense small cells from channel measurements," in *Proc. IEEE 83rd Veh. Technol. Conf. (VTC Spring)*, May 2016, pp. 1–5.

[12] M. G. Sarret, M. Fleischer, G. Berardinelli, N. H. Mahmood, P. Mogensen, and H. Heinz, "On the potential of full duplex performance in 5G ultra-dense small cell networks," in *Proc. 24th Eur. Signal Process. Conf. (EUSIPCO)*, Aug. 2016, pp. 764–768.

[13] D. López-Pérez, M. Ding, H. Claussen, and A. H. Jafari, "Towards 1 Gbps/UE in cellular systems: Understanding ultra-dense small cell deployments," *IEEE Commun. Surveys Tuts.*, vol. 17, no. 4, pp. 2078–2101, 4th Quart., 2015.

[14] *Evolved Universal Terrestrial Radio Access (E-UTRA); Small Cell Enhancements for E-UTRA and E-UTRAN—Physical Layer Aspects, Rel.12 v12.1.0*, document 3GPP TSG RAN TR 36.872, 2013.

[15] M. Z. Win, P. C. Pinto, and L. A. Shepp, "A mathematical theory of network interference and its applications," *Proc. IEEE*, vol. 97, no. 2, pp. 205–230, Feb. 2009.

[16] O. Galinina, A. Pyattaev, S. Andreev, M. Dohler, and Y. Koucheryavy, "5G multi-RAT LTE-WiFi ultra-dense small cells: Performance dynamics, architecture, and trends," *IEEE J. Sel. Areas Commun.*, vol. 33, no. 6, pp. 1224–1240, Jun. 2015.

[17] K. Lee, Y. Park, M. Na, H. Wang, and D. Hong, "Aligned reverse frame structure for interference mitigation in dynamic TDD systems," *IEEE Trans. Wireless Commun.*, vol. 16, no. 10, pp. 6967–6978, Oct. 2017.

[18] B. Yu, L. Yang, H. Ishii, and S. Mukherjee, "Dynamic TDD support in macrocell-assisted small cell architecture," *IEEE J. Sel. Areas Commun.*, vol. 33, no. 6, pp. 1201–1213, Jun. 2015.

[19] J. G. Andrews, F. Baccelli, and R. K. Ganti, "A tractable approach to coverage and rate in cellular networks," *IEEE Trans. Commun.*, vol. 59, no. 11, pp. 3122–3134, Nov. 2011.

[20] J. F. C. Kingman, *Poisson Processes* (Oxford Studies in Probability). Oxford, U.K.: Clarendon, 1992. [Online]. Available: https://books.google.co.kr/books?id=VEiM-OtwDHkC

[21] M. Chung, M. S. Sim, J. Kim, D. K. Kim, and C.-B. Chae, "Prototyping real-time full duplex radios," *IEEE Commun. Mag.*, vol. 53, no. 9, pp. 56–63, Sep. 2015.

[22] M. Heino *et al.*, "Recent advances in antenna design and interference cancellation algorithms for in-band full duplex relays," *IEEE Commun. Mag.*, vol. 53, no. 5, pp. 91–101, May 2015.

[23] O. Vermesan and P. Friess, *Internet of Things: Converging Technologies for Smart Environments and Integrated Ecosystems*. Aalborg, Denmark: River Publishers, 2013.

[24] J. Lee, J. G. Andrews, and D. Hong, "Spectrum-sharing transmission capacity," *IEEE Trans. Wireless Commun.*, vol. 10, no. 9, pp. 3053–3063, Sep. 2011.

[25] J. Lee and T. Q. S. Quek, "Hybrid full-/half-duplex system analysis in heterogeneous wireless networks," *IEEE Trans. Wireless Commun.*, vol. 14, no. 5, pp. 2883–2895, May 2015.

HAESOON LEE (S'12) received the B.S. degree in electrical and electronic engineering from Yonsei University, Seoul, South Korea, in 2012, where he is currently pursuing the joint M.S./Ph.D. degree in electrical and electronic engineering. His current research interests include 5G wireless communications. In addition, his current research interest is the performance improvement of full duplex system and cellular-based V2X communications.

YOSUB PARK (S'11–M'18) received the B.S. and Ph.D. degrees in electrical and electronic engineering from Yonsei University, Seoul, South Korea, in 2011 and 2018, respectively. Since 2018, he has been a Senior Engineer with the Autonomous Machine Laboratory, AI Center, Samsung Research, Samsung Electronics Company, Seoul. His research interests are in 5G/6G wireless communications, such as ultra-dense networks and cellular-based V2X communications. In addition, his current research interests include the simulator design and development for autonomous driving systems and new waveform design issues, such as FBMC, GFDM, and F-OFDM.

DAESIK HONG (S'86–M'90–SM'05) received the B.S. and M.S. degrees in electronics engineering from Yonsei University, Seoul, South Korea, in 1983 and 1985, respectively, and the Ph.D. degree from the School of EE, Purdue University, West Lafayette, IN, USA, in 1990. He joined Yonsei University in 1991, where he is currently a Professor with the School of Electrical and Electronic Engineering. He has been serving as the Chair of the Samsung-Yonsei Research Center for Mobile Intelligent Terminals. He also served as a Vice-President of the Research Affairs and the President of the Industry-Academic Cooperation Foundation, Yonsei University, from 2010 to 2011. He was appointed as the Underwood/Avison Distinguished Professor with Yonsei University in 2010. He also served as a Chief Executive Officer for Yonsei Technology Holding Company in 2011, and served as the Vice President of the Institute of Electronics and Information Engineers from 2012 to 2015. He currently serves as the Dean of the College of Engineering with Yonsei University. His current research activities are focused on the future wireless communication, including 5G systems, OFDM(A) and multi-carrier communication, multi-hop and relay-based communication, in-band full-duplex, cognitive radio, and energy harvesting.

Dr. Hong received the Best Teacher Award at Yonsei University in 2006, 2010, and 2012. He was also a recipient of the HaeDong Outstanding Research Awards from the Korean Institute of Communications and Information Sciences in 2006 and the IEIE in 2009. He served as an Editor for the IEEE Transactions on Wireless Communications from 2006 to 2011. He currently serves as an Editor for the IEEE Wireless Communications Letters.